Progress In Electromagnetics Research M, Vol. 55, 13–24, 2017

Calculating Radar Cross Section of Lossy Targets Using the Surface Impedance Approach

El M. Hamham[1, *], Asmaa Zugari[2], and Abdelilah Benali[3]

Abstract—In this paper, an effective numerical method based on a new surface impedance model is applied to the accurate calculation of the radar cross section of lossy conducting targets. The problem of determining the scattered electromagnetic fields from rectangular lossy conducting strips is presented and treated in detail. This problem is modeled by the method of moments to resolve integral equations of the first kind of surface current density with an accurate choice of basis and test functions. The illustrative computation results of complex surface impedance, surface current density and radar cross section are given for several cases. The accuracy of the method presented in this paper is verified by comparison with other methods, including the general-purpose full-wave simulators HFSS and CST.

1. INTRODUCTION

When a perfectly conducting target is illuminated by an electromagnetic field, electric currents are induced on the surface of the body. These currents act as new sources and create an electromagnetic field radiated outward from the body. This field, called the scattered field, depends on the frequency and the polarization of the incident field. The scattered field is also related to the physical dimensions and shape of the illuminated body [1]. In real conducting body with finite conductivity illuminated with an electromagnetic field, the fields extend into the conductor, but decrease rapidly with distance from the surface due to the well-known skin effect. According to the ratio between the wavelength of the incident field and the illuminated body size, at least three scattering regimes can be defined [2]. These are: Low-frequency scattering, resonant scattering and high frequency scattering. The spatial distribution of the power of the scattered field is characterized with radar cross section, or RCS as it is commonly referred to in literature, which is a fictitious area of the target [3–10]. For simple scattering bodies, the RCS can be computed exactly by a solution of the wave equation in a coordinate system for which a constant coordinate coincides with the surface of the body [1, 2]. The exact solution requires that the electric and magnetic fields just inside and just outside the surface satisfy certain conditions that depend on the electromagnetic properties of the material of which the body is made. However, for complex scattering bodies an alternative techniques based on the solution of the integral equations governing the distribution of induced fields on the conducting target surfaces are used. These computational techniques can be classified into two groups, the exact and approximate solution techniques. The exact methods, as the Method of Moments (MoM) and the Finite Elements Method (FEM), are rigorous solutions based on the integral and differential equations, respectively. However, some approximations may be performed when solving the integral or differential equations by numerical techniques. The most useful approach to solution is known as the method of moments which is a numerical technique [11–14] used to approximately solve a system of linear homogeneous equations such as differential equations or integral

Received 15 October 2016, Accepted 8 February 2017, Scheduled 22 February 2017
* Corresponding author: El Mokhtar Hamham (elm.hamham@gmail.com).
[1] Department of Applied Physics, University of Salamanca, Edificio Trilingüe Plaza de la Merced s/n, Salamanca 37008, Spain. [2] EMG Group, Department of Physics, Abdelmalek Essaadi University, BP. 2121, Tetouan 93030, Morocco. [3] Dpto. Enginería Electronica, Universidad Autonoma de Barcelona, Bellaterra, Barcelona 08193, Spain.

equations. The unknown function is approximated by a finite series of known expansion functions with unknown expansion coefficients. The approximate function is substituted into the original operator equation and the resulting approximate equation is tested so that the weighted residual is zero. This results into a number of simultaneous algebraic equations for the unknown coefficients. These equations are then solved using matrix calculus. The method of moments has been used to solve a vast number of EM problems during the last decades. The main advantage of the method of moments in the calculation of the scattered fields is that the surface profile of the target body is unrestricted, allowing the computation of the scattering from complex objects.

In this paper, we make use of the Galerkin's method, that is a variant of the method of moments, together with the surface impedance approach to calculate the RCS of an infinite lossy resistive rectangular conducting strip in quasi Transverse Electromagnetic (TEM) frequency limit. Hence, we present the procedures application of a recent version of the surface impedance technique for the calculation of the induced current and the scattered field on the surface of a resistive conducting target illuminated by an incident TM polarized field. If the source illuminating the target is at a far enough distance, then the incident field can be taken as a plane wave. The surface impedance technique used in this study has been developed in [15] for the calculation of conductor loss of single and two coupled rectangular microstrip lines. The accuracy of this technique has been improved recently in [16] for three, four and five coupled conducting strips embedded in a lossless dielectric medium. The main advantage of this technique, based on quasi-TEM approximations, is the simplicity to deal with rectangular resistive targets taking into account the thickness of the conductor and edge currents. As it is well known, when a body is illuminated by a plane wave, the current is induced on its surface. However, around the edges of the body this current has more complicated behavior, due to the diffraction of the incident field. The edge diffracted field appears to come from a nonuniform line source located at the edge [1]. The bad estimation of the edge current could affect the calculation of the RCS. The most of the works studying lossy targets consider the later as a resistive conducting sheet. A resistive sheet is a special case of the surface impedance since it does not support magnetic currents. In this case, they use an estimation of the sheet resistivity [13, 17, 18]. In this work, we calculate the complex surface impedance by making use of a good approximation. The solution yields the surface impedance at every point on the surface of the body for a specified scattered field (or RCS) pattern. Once the surface impedance is known, the electrical properties of the material can be determined. Therefore, in this paper we proceed as follow: firstly we give a brief review of the basic elements in the analysis of rectangular conducting strip as well as the fundamental concepts relative to the wave propagation under quasi-TEM approach and surface impedance technique. Then, we present a detailed description of the application of Galerkin's method for the resolution of the surface current density integral equation by making use of adequate triangular basis and test functions. Finally, we present the illustrative computation results of the surface impedance, the surface current density, and the RCS for several cases. It is shown that the obtained numerical results and those obtained with full wave commercial simulators are in good agreement.

2. CALCULATING THE RCS OF THE LOSSY TARGETS

The RCS of a target is defined isotropically as the ratio of the reflected power to the incident power density. A general expression is given by

$$\sigma(\phi) = \lim_{R\to\infty} 4\pi R^2 \frac{|\mathbf{E}^{scat}|^2}{|\mathbf{E}^{inc}|^2}, \tag{1}$$

where $\mathbf{E}^{inc}$ is the electric field strength of the incident wave impinging on the target, and $\mathbf{E}^{scat}$ is the electric field strength of the scattered wave at the radar. The derivation of the expression assumes that a target extracts power from an incident wave and then radiates that power uniformly in all directions. R is typically taken to be the range from the radar to the target, and ϕ is the observation angle. Also, it is possible to define a logarithmic quantity with respect to the RCS, so that

$$\sigma_{\mathrm{dB}sm} = 10\log_{10}\sigma/1m^2. \tag{2}$$

The incident field that impinges on the surface of the target induces on it an electric current density, J_s, which in turn radiates the scattered field. The scattered field everywhere can be found using the

following equation [1, 19]:

$$\mathbf{E}(\mathbf{r})^{scat} = -j\omega\mathbf{A} - j\frac{1}{\omega\mu\epsilon}\boldsymbol{\nabla}(\boldsymbol{\nabla}\cdot\mathbf{A}), \tag{3}$$

where, A is the magnetic vector potential, $\boldsymbol{\nabla}$ the gradient operator, ω the angular frequency of the incident field, ϵ the permittivity of the medium, and μ the permeability of the medium. The magnetic vector potential can be found using the following equation [1, 19]:

$$\mathbf{A} = \frac{\mu}{4\pi}\iint_S \mathbf{J}_s(\mathbf{r}')\frac{\exp^{-jkR}}{R}dS', \tag{4}$$

where, R is the distance from the source point to the observation point. On the other hand, for the perfect electric conductor (PEC), the total field on the surface of the target is zero. However, for real conductor (with finite conductivity), the total field on the surface of the scatterer is determined by the following boundary condition:

$$\mathbf{E}_t^{total} = -Z_s\mathbf{J}_s, \tag{5}$$

where, t stands for tangential components to the surface of the conductor, Z_s the surface impedance, and J_s the surface current density.

The total field on the surface of the conductor, S, can be expressed as

$$\mathbf{E}_t^{total}(\mathbf{r}=\mathbf{r}_s) = \mathbf{E}_t^{scat}(\mathbf{r}=\mathbf{r}_s') + \mathbf{E}_t^{inc}(\mathbf{r}=\mathbf{r}_s), \tag{6}$$

where, $\mathbf{r}=\mathbf{r}_s$ is the position vector of any point on the surface of the conductor target.

If the observations are restricted on the surface of the target, substituting Eq. (4) in Eq. (6) and using the surface boundary condition (Eq. (5)) one can obtain the following expression:

$$j\frac{\eta}{k}\left[k^2\iint_S \mathbf{J}_s(\mathbf{r}')\,G(\mathbf{r}_s,\mathbf{r}')dS' + \nabla\iint_S \nabla'\cdot\mathbf{J}_s(\mathbf{r}')\,G(\mathbf{r}_s,\mathbf{r}')dS'\right] + Z_s(\mathbf{r}=\mathbf{r}_s)\mathbf{J}_s(\mathbf{r}=\mathbf{r}_s) = -\mathbf{E}_t^{inc}, \tag{7}$$

where, $\eta = \sqrt{\dfrac{\mu}{\epsilon}}$ is the intrinsic impedance of the medium; $k = \omega\sqrt{\mu\epsilon}$ is the phase constant; $\mathbf{r}$ and $\mathbf{r}'$ are the position vectors of the observation point and source point respectively, and $R = |\mathbf{r}-\mathbf{r}'|$. With $G(\mathbf{r},\mathbf{r}')$ being the Green's function of the three dimensional target:

$$G(\mathbf{r},\mathbf{r}') = \frac{\exp^{-jkR}}{4\pi R}. \tag{8}$$

Eq. (7) is referred as Electric Field Integral Equation (EFIE). It is a general three-dimensional surface boundary condition that can be simplified for the structure studied in this work (bidimensional).

3. RESOLUTION OF THE ELECTRIC FIELD INTEGRAL EQUATION

The assumptions that we will take into account are essentially quasi-TEM fields outside the conductor strip and TM fields inside; that is,

$$\begin{array}{ll} H_z = 0, & \text{on all the structure} \\ \mathbf{E}_t^c = 0, & \text{on the conductor} \\ \mathbf{A}_t = 0, & \text{on the conductor} \\ \nabla\times\mathbf{E}_t^d = 0, & \text{outside the conductor} \\ \nabla\times\mathbf{H}_t^d = 0, & \text{outside the conductor.} \end{array} \tag{9}$$

From the above assumptions together with Maxwell's equations, we can obtain the electromagnetic fields wave equations on the conductors with the condition of good conductor ($\sigma_c \gg \omega\varepsilon$) as

$$(\nabla_t^2 - \mathrm{j}\omega\mu_0\sigma_c)\mathbf{H}_t^c = 0, \tag{10}$$

$$(\nabla_t^2 - \mathrm{j}\omega\mu_0\sigma_c)E_z^c = 0, \tag{11}$$

where, subscripts c, z and t stand for conductor, longitudinal z-direction and transversal component, respectively. μ_0 is the free space permeability, and σ_c is the strip conductivity.

According to the assumptions made above Eq. (9), only the electric transversal components are relevant outside the conductors, and only the electric longitudinal components are relevant inside the conductors ($\mathbf{E}_t^c = 0$). Thus, from Eq. (3), Eq. (9), and Maxwell's equations, the relations that relate the fields to the potentials inside the conductors can be reduced to

$$\mathbf{H}_t = \frac{1}{\mu_0}\hat{\mathbf{z}} \times \nabla_t A_z, \tag{12}$$

$$E_z = -\mathrm{j}\omega A_z, \tag{13}$$

where A_z is the magnetic potential component in the direction of propagation.

Then, from Eq. (11) and Eq. (13) we can obtain the potential vector wave equation inside the conductor that can be written as:

$$(\nabla_t^2 - \mathrm{j}\omega\mu_0\sigma_c)A_z = 0. \tag{14}$$

Outside the strip, the magnetic potential vector wave equation is the Laplace equation

$$\nabla_t^2 A_z = 0, \tag{15}$$

with the boundary condition $A_z = Cte$, on the strip.

At this point it should be recognized that the electromagnetic problem remains magnetostatic outside the conductors (Eq. (15)) and reduces to the diffusion equation (Eq. (14)) inside the conductors.

The rigorous computation of the total currents in the conductors implies the resolution of Eq. (14) inside the conductors. Moreover, the resolution of the differential equation of the structure under study Eq. (14) is not trivial. To circumvent these constraints, Marqués et al. have proposed an alternative approximated method making use of the *surface impedance* concept [20, 21]. Recently, this concept has been improved in [15, 16] by making use of a new calculation strategy.

3.1. Surface Impedance

For an ideal conductor in an EM field, the tangential component of the electric field at the surface is zero. A current flows in a thin sheet on the surface, as required to support the magnetic field tangential to the surface. This short-circuit boundary condition excludes all fields from the interior of the ideal conductor. In a real conductor, the fields extend into the conductor, but decrease rapidly with distance from the surface (skin effect). To avoid the complication of solving Maxwell's equations inside conductors, it is usual to make use of the concept of surface impedance. The surface impedance provides the boundary condition for fields outside the conductor and accounts for the dissipation and energy stored inside the conductor. The main idea of the surface impedance approach in the study of microstrip lines with rectangular cross section, as presented in [15, 20], is to replace the thick conducting strip with a zero-thickness sheet that carries an equivalent surface current density, J_s. The main advantage of this technique is to avoid the solution of a wave equation for the potential vector inside the thick strip (Eq. (14)). The equivalent surface current density, J_s, can be linearly related to the value of the electric field longitudinal component, E_z, at the surface of zero-thickness resistive conductor strip as

$$E_z(x) = Z_s J_s(x), \tag{16}$$

where Z_s is the complex surface impedance of the conductor.

The calculation of Z_s may be estimated a priori by an approximate phenomenological model that takes into account the thickness of the conductor, the finite conductivity and other characteristics of the structure. Otherwise it can be obtained numerically. In the next section we will present an existing approximated model and we will develop an accurate quasi-TEM approach for the efficient numerical computation of Z_s.

The surface boundary condition in Eq. (16) along with Eq. (13) allows us to write

$$A_z(x) = \frac{\mathrm{j}}{\omega} Z_s J_s(x). \tag{17}$$

3.2. Numerical Computation of Surface Impedance

The choice of the surface impedance introduced in the above equations can be done in many different ways. One of those methods is the technique proposed by [20], which has been improved recently in [15, 16]. The main advantage of this technique is that it can be combined with a quasi-TEM approach to form the so-called quasi-TEM surface impedance approach.

We consider the thick resistive strip that is very long in the Z-direction of Fig. 1(a). According to the surface impedance technique, this thick strip is substituted by a zero-thickness one that carries a surface current density J_s and a surface impedance Z_s. The new approximate equivalent structure is shown in Fig. 1(b). To obtain the surface impedance of this equivalent structure, we proceed as detailed in [15]:

$$Z_s = \frac{\Delta}{\sigma_c}\left[\frac{1+\Gamma}{1-\Gamma}\coth(\Delta t) - \frac{\Gamma}{1-\Gamma}\coth(\Delta t/2)\right], \tag{18}$$

where $\Gamma = H_x^+/H_x^-$ is the ratio between the tangential magnetic fields, H_x, on the upper ($^+$) and lower ($^-$) interfaces of the conducting strip, $\Delta = (1+\mathrm{j})/\delta$; δ is the skin depth in the metal, σ is the metal conductivity; t is the metalization thickness. Thus, for the calculation of the ratio H_x^+/H_x^- we follow the method proposed in [15]. This strategy results in a direct semi-numerical calculation and a faster CPU time. For this purpose, we solve the following auxiliary magnetic quasi-static problem for the structure in Fig. 1(b):

$$\begin{cases} \nabla_t^2 A_z = 0, & \text{outside the strip} \\ A_z = A_0, & \text{on the strip} \end{cases} \tag{19}$$

where A_z is the longitudinal component of the potential vector; subscript t stands for transverse (to z) components; A_0 is an arbitrary constant. In order to solve the differential Eq. (19), we use the Galerkin's version of the method of moments. In this case, Eq. (19) is transformed into the following integral equation for the surface current density, J_z, on the zero-thickness perfect conductor strip ($-W/2 \le x \le W/2$) located at $y = 0$ (see Fig. 1(b)):

$$A_z[J_s] = A_0, \tag{20}$$

where

$$A_z[J_s] = \mu_0 \int_{-W/2}^{W/2} J_z(x')\, G(x-x')\, \mathrm{d}x', \tag{21}$$

with $G(x-x')$ being the Green's function for the two dimensional free space problem on the conductor strip surface ($y = 0$). This function can be written in the spatial domain as follows [12]:

$$G(\mathbf{r}-\mathbf{r}') = -\frac{1}{4j} H_0^{(2)}(k|\mathbf{r}-\mathbf{r}'|), \tag{22}$$

where, $k = 2\pi/\lambda$ is the free space wave number, λ the wave length, $\mu_0 = 4\pi \times 10^{-7}$ the free space permeability, and $H_0^{(2)}$ a Hankel function of the second kind of zero order. According to the method

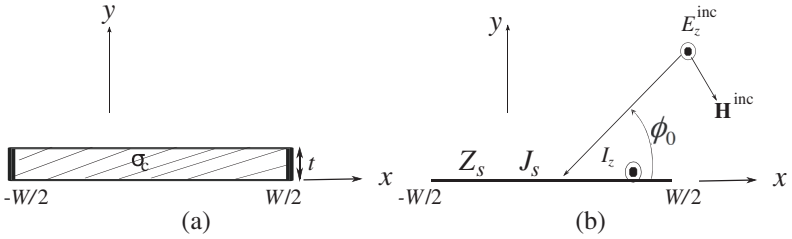

Figure 1. The structure under study: (a) A lossy strip with width, W, thickness, t, and conductivity, σ_c, is encountered (illuminated) by an incoming TM-polarized plane wave. (b) Zero-thickness equivalent structure with surface impedance Z_S and surface current density J_S. ϕ_0 is the incident angle taking the strip center as the origin of angles.

of moments, the surface current density is approximated by a finite set of basis functions on the strip surface. For a convenient description of the strip edge effects, as explained and detailled in [15, 20], J_z is expanded in terms of Chebyshev polynomials weighted with the Maxwell edge distribution. Once the unknown coefficients of the J_z expansion are computed, we can use Eq. (21) to obtain the longitudinal vector potential, $A_z(x, y)$. The tangential magnetic field can finally be computed as

$$H_x(x, y) = \frac{\partial A_z(x, y)}{\partial y}, \tag{23}$$

and the values at the lower and upper strip interfaces of the zero-thickness strip are then given by

$$H_x^-(x) = H_x(x, 0^-), \tag{24}$$

$$H_x^+(x) = H_x(x, t), \tag{25}$$

where 0^- indicates an infinitesimal distance below $y = 0$ (see Fig. 1).

Finally we use the following definition of Γ:

$$\Gamma = \frac{H_x^+(0)}{H_x^-(0)}, \tag{26}$$

where $x = 0$ stands for the center of the strip. Once we have the numerical value of Γ computed from Eq. (26), it is introduced into Eq. (18) to obtain the corresponding surface impedance, Z_s. At this stage, the resolution of the lossless magnetic problem in Eq. (19) has been done to obtain the surface impedance (Z_s) that models the finite-conductivity of the strip. The next step is to introduce Z_s in the *lossy* magnetic problem and to solve the corresponding integral equation for the new surface current density, $J_z^{(\sigma_c)}$, using the Galerkin's method.

3.3. Lossy Rectangular Strip

For lossy zero-thickness strip, the integral equation for the current density defined in Eq. (17) can be rewritten as

$$\omega A_z[J_s^{(\sigma_c)}] - \mathrm{j} Z_s J_s^{(\sigma_c)} = 0 \,, \tag{27}$$

where $A_z[J_s^{(\sigma_c)}]$ is defined in Eq. (21). In order to solve the integral Eq. (27), we apply the Galerkin's method and Parseval's identity. Thus, we approximate the surface current density on the conductor strip as the following finite sum of N_f basis functions, J_n,

$$J_s^{(\sigma_c)}(x) = \sum_{n=0}^{N_f} \alpha_n J_n(x). \tag{28}$$

As we have mentioned before, one of the most important criteria that one should take it into account in the choice of basis and test functions is the convergence of the involved reaction integrals. In this sense, to approximate the surface current density for the case of lossy conductor strip, one could choose the same basis and test functions as in the case of the calculation of the surface impedance in the zero-thickness strip, i.e., the Chebyshev polynomials weighted with the Maxwell's edge distribution. However, this choice is not adequate because it leads to divergent integrals. Therefore, we use the subdomain triangular basis and test functions which can be written in the spatial domain as

$$J_0 = \begin{cases} \dfrac{x_1 - x}{x_1 - x_0}; & x_0 < x < x_1 \\ 0 & \text{elsewhere} \end{cases} \tag{29}$$

$$J_i = \begin{cases} \dfrac{x - x_i}{x_i - x_{i-1}}; & x_{i-1} < x < x_i \\ \dfrac{x_{i+1} - x}{x_{i+1} - x_i}; & x_i < x < x_{i+1} \\ 0 & \text{elsewhere} \end{cases} \tag{30}$$

$$J_{N_f} = \begin{cases} \dfrac{x - x_{N_f-1}}{x_{N_f} - x_{N_f-1}}; & x_{N_f-1} < x < x_{N_f} \\ 0 & \text{elsewhere} \end{cases} \tag{31}$$

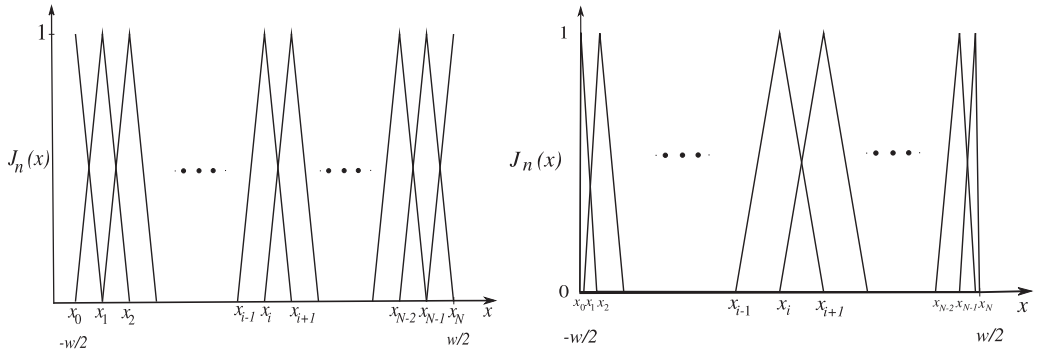

Figure 2. Triangular basis functions. (a) Uniform distribution. (b) Nonuniform distribution.

Fig. 2(a) illustrates the triangular impulses uniformly distributed along a conductor strip width. However, the choice of basis and test functions is based on experience more than other criteri. In this sense, we find that the triangular expansion functions used in this work as defined in Eq. (29)– Eq. (31) and illustrated in Fig. 2(a) lead to a bad approximation of the surface current density when the distribution elements, x_i, are equally or uniformly spaced,

$$x_i = -\frac{W}{2} + \frac{i}{N_f}W, \quad i = 0, 1, 2, \ldots, N_f. \tag{32}$$

To overcome this constraint, we use a nonuniform distribution based on sinusoidally spaced elements defined as

$$x_i = \frac{W}{2}\sin\left(\frac{2i - N_f}{2N_f}\pi\right), \quad i = 0, 1, 2, \ldots, N_f. \tag{33}$$

These nonuniform triangular functions are illustrated in Fig. 2(b). Finally, the total current on the conducting strip is given by integrating the surface current density along the strip width as follows

$$I_z = \int_{-W/2}^{W/2} J_s^{(\sigma_c)}(x)\,\mathrm{d}x. \tag{34}$$

4. NUMERICAL RESULTS AND DISCUSSION

We start the numerical analysis as we have done above. First of all, we give the numerical results of the surface impedance calculation for the more significant parameters of the structure obtained by the use of the zero-thickness technique.

In Fig. 3, we plot the variation of the real and imaginary parts of the surface impedance, that is, the resistance and reactance, as function of the strip thickness for different frequencies. As can be seen, for different frequencies and as long as the thickness increases, the effect of the imaginary part that contributes to the conducting losses becomes as important as the real part. In addition, for high frequencies this effect becomes more noticeable even for thin conducting strip. This behavior is due to the skin depth.

To show the dependence of the surface impedance on the skin depth, we plot in Fig. 4 the variation of the resistance and reactance of the conducting strip as a function of the strip conductivity for different thicknesses. The static resistance, R_s defined bellow, is also reported for comparison

$$R_s = \sqrt{\frac{\omega\mu_0}{2\sigma_c}}. \tag{35}$$

As can be seen, the behavior of the real and imaginary parts of the surface impedance changes as the thickness of the conductor strip is increased. As expected, the surface resistance (real part) is inversely

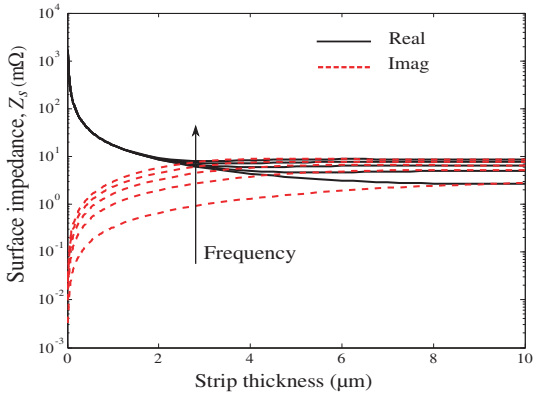

Figure 3. Real and imaginary parts of surface impedance as function of the conducting strip thickness for different frequencies. $W = 6\lambda$, $\sigma_c = 4 \times 10^7$.

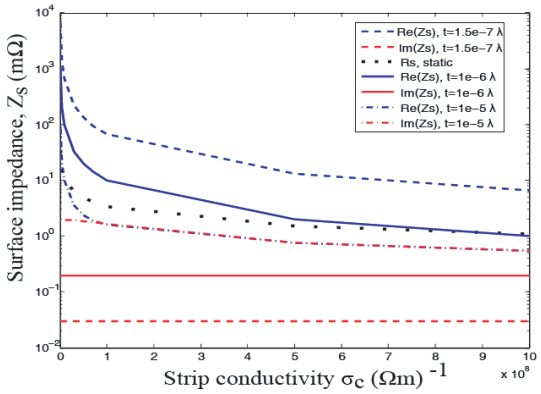

Figure 4. Real and imaginary parts of surface impedance as function of the conductivity for different thickness with $W = 6\lambda$ and frequency = 0.3 GHz.

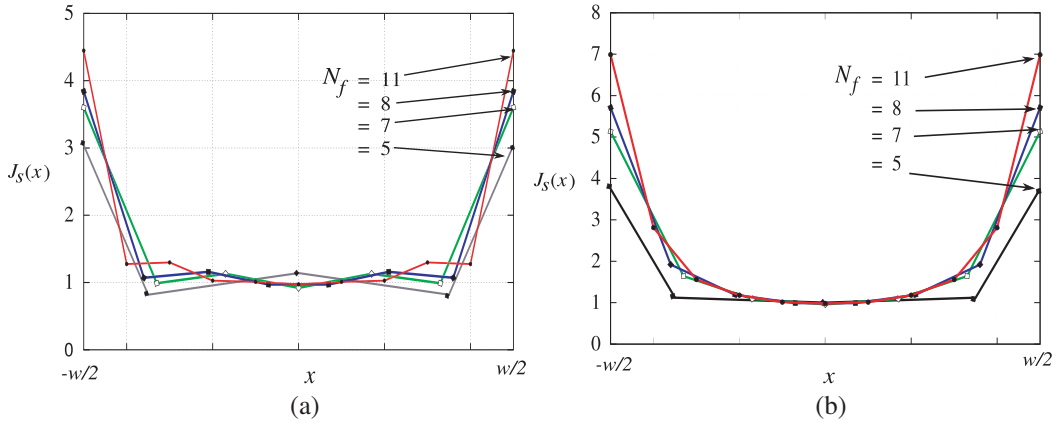

Figure 5. The distribution of surface current density along the strip width obtained using triangular basis functions. (a) Uniformly spacing. (b) Sinusoidally spacing. Strip thickness, $t = 5\,\mu$m, Frequency = 0.3 GHz, $\sigma_c = 5.8 \times 10^7$.

proportional to the variation of both thickness and strip conductivity. However, the surface reactance (imaginary part) remains constant for thin strips for all the conductivity values and follows the same behavior as the surface resistance for thick strips. The discrepancy in values between our results for the surface resistance and the static one is due to the fact that the static surface resistance is based on the approximation of a lossless strips and then it is independent of the metal thickness. Once the surface impedance is calculated, we can solve the integral equation for the surface current density. The results are shown in Fig. 5. There, we plot the approximated distribution of the surface current density, J_s, along the cross section of a rectangular conducting strip using both uniform and nonuniform triangular functions in order to show the difference between them. As can be seen, the sinusoidally spaced triangular functions give a good approximation of the surface current density in comparison with the uniformly spaced functions. Moreover, when equally spaced basis and test functions are used the approximate surface current density functions oscillate around the conducting strip center. However, when the sinusoidal functions are used, the surface current density functions smoothly converge to their limiting form as the number of the basis and testing functions increases. By integrating along the conducting strip width, we can obtain the total current.

In Fig. 6, we show the magnitude of the current distribution across the surface of the conducting strip for different thicknesses. It can be seen that the current distribution is strongly dependent on the

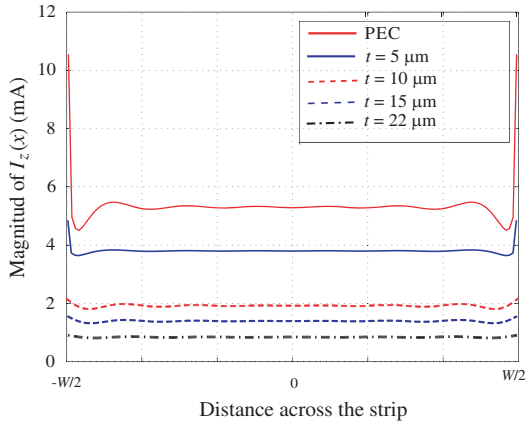

Figure 6. The magnitude of the current distribution across the surface of the lossy strip for different thicknesses. $W = 6\lambda$, Frequency $= 0.3$ GHz, $\sigma_c = 5.8 \times 10^7$.

Table 1. The comparison of RCS maxima for different conducting strip widths as calculated in Fig. 7.

	This work	HFSS	CST	Approx.
$W = 1 \times \lambda$	11.49	11.22	10.63	11.41
$W = 2 \times \lambda$	16.96	17.09	18.81	16.94
$W = 4 \times \lambda$	23.46	23.08	25.44	23.46
$W = 6 \times \lambda$	26.69	26.61	29.19	26.67

strip thickness. The result for a perfect electrically conducting (PEC) strip is reported for comparison. The results for the PEC case are obtained by taking $Z_s = 0$ directly or σ_c very high in our numerical model. The dependence of the current distribution on the strip thickness in Fig. 6 is related to the surface impedance as it has been shown before.

We should note that, as can be seen from Fig. 6, for the PEC case the current presents singularity at the conducting strip edges. This is because the triangular basis functions are not adequate for the approximation of the currents at the lossy strip edges. For this reason, as explained in Section 3.1, we use the Chebyshev polynomials weighted with Maxwell's edge distribution to deal with lossless problem. To illustrate the proposed model, to validate the accuracy of the approach presented in this work and to better demonstrate the utility of the presented method for the calculation of the RCS, we report in Fig. 7(a)–Fig. 7(d) the results of the bistatic RCS (BRCS) of a lossy conducting strip as a function of the observation angle for different strip width. Our results are compared with those obtained using a previous method based on an analytical approximation of the surface impedance [20], and the full wave simulators HFSS and CST. These results show that the maximum of the RCS magnitude is proportional to the conducting strip width. As wide as the conducting strip, the magnitude of the RCS increases. The excellent agreement is observed between our results and those obtained by HFSS. However, it can be seen that the maximums of RCS obtained by our approach and HFSS differ slightly from the results obtained by CST. This is may due to the method used in CST to calculate the far-field components. A quantitative comparison of the maximum of RCS values for different conducting strip widths is reported in Table 1.

In Fig. 8, we plot the results of the monostatic RCS as a function of the aspect (observation) angle of a 6-λ rectangular conducting strip with different thicknesses. We also report the results of PEC strip which we compare with those obtained making use of the HFSS software. It is easily seen from the figure that our results show a good agreement with those obtained with HFSS for the PEC case. For the other cases, we omit HFSS results for the clarity of the figure. As expected, we can see that when the strip is thicker, the maximum of the RCS decreases. Also, it is observed that the

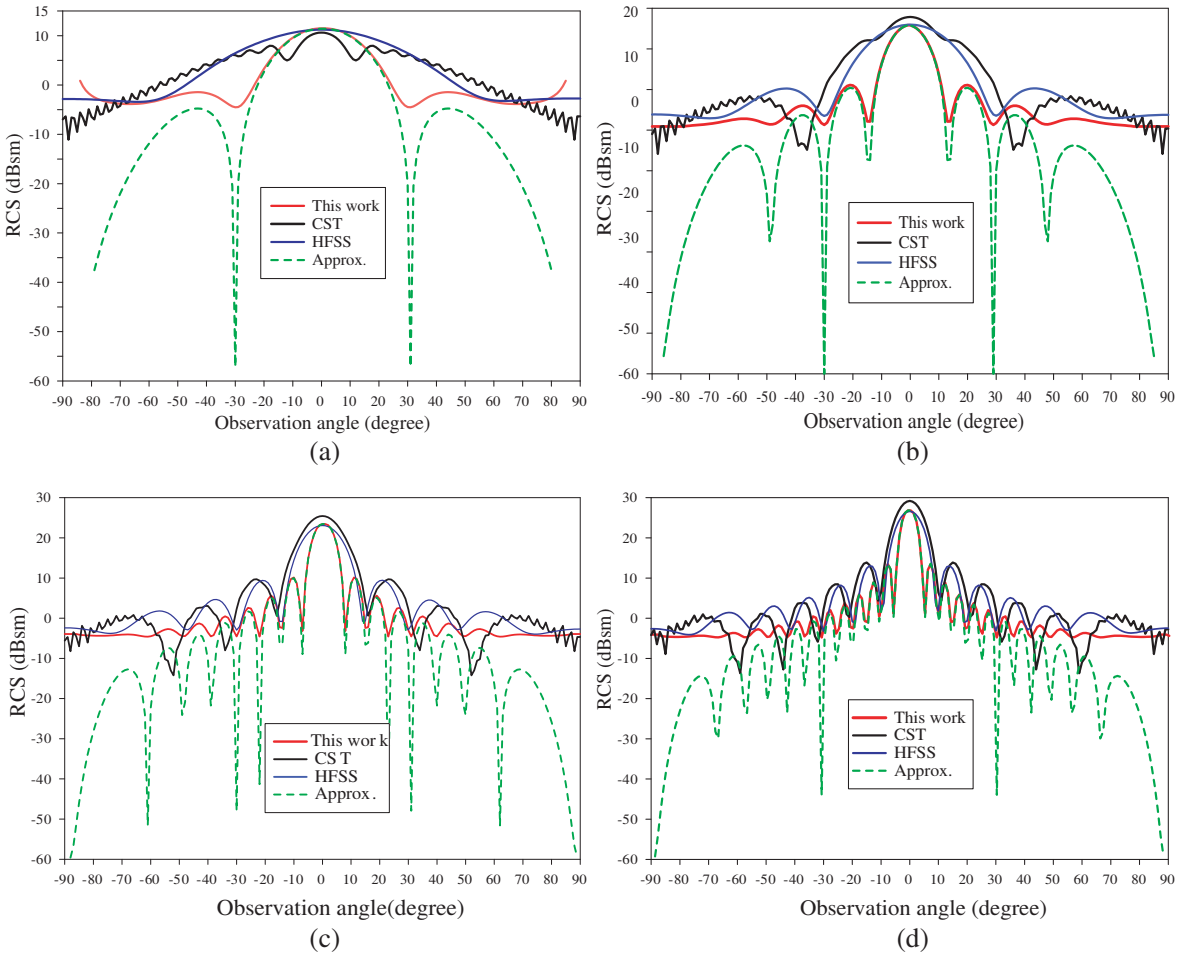

Figure 7. Bistatic RCS of a strip as a function of the observation angle for different widths. (a) $W = \lambda$. (b) $W = 2\lambda$. (c) $W = 4\lambda$. (d) $W = 6\lambda$. Frequency $= 0.3\,\text{GHz}$, $\sigma_c = 5.8 \times 10^7$, $\phi_0 = \pi/2$.

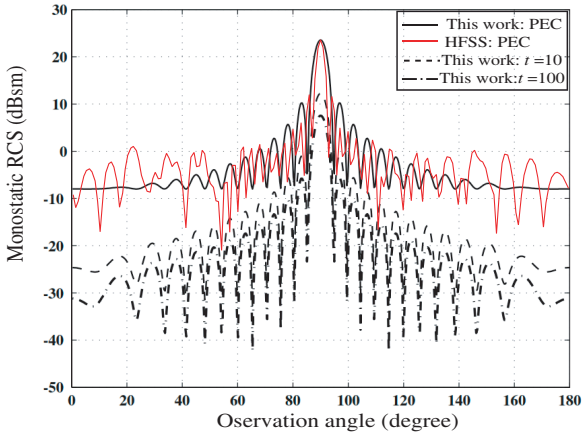

Figure 8. The monostatic RCS of a lossy rectangular strip for different thicknesses. $W = 6\lambda$, Frequency $= 0.3\,\text{GHz}$, $\sigma_c = 5.8 \times 10^7$, $\phi_0 = \pi/2$. The thickness, t, is in μm.

RCS decreases with respect to the PEC case. In the light of the numerical results presented above, the stability and accuracy of the numerical code based on the methods used in this study has been verified. The good agreement of the results obtained by our surface impedance model with those provided by

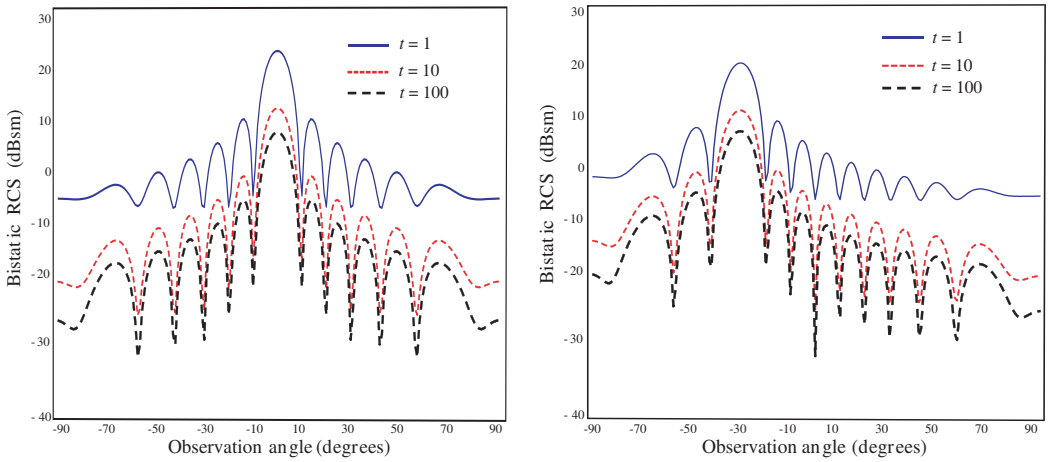

Figure 9. The bistatic RCS of a lossy strip of width $W = 6\lambda$ for different strip thickness, t, in μm, $\sigma_c = 5.8 \times 10^7$. (a) $\phi_0 = \pi/2$. (b) $\phi_0 = 3\pi/2$.

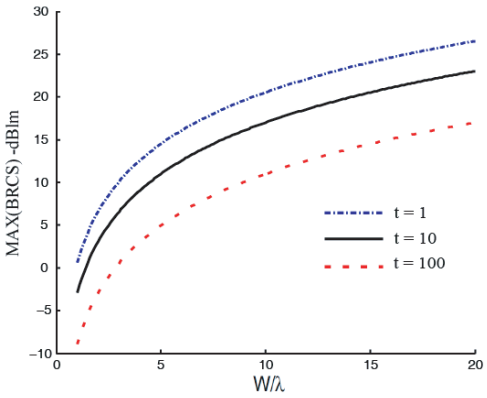

Figure 10. The maximum of the BRCS as function of the strip width for different thicknesses. Frequency = 0.3 GHz, $\sigma_c = 5.8 \times 10^7$. The thickness, t, is in μm.

more involved full-wave electromagnetic simulators shows the generality of the model and its utility in the calculation of the RCS. To complete the study, in Fig. 9 we plot the BRCS versus the observation angle of a lossy rectangular strip for different strip thicknesses and incident angles. Thus, in Fig. 9(a) and Fig. 9(b) we show the variation of BRCS for horizontal incidence ($\phi_0 = \pi/2$) and for oblique incidence ($\phi_0 = 3\pi/2$), respectively. It can be seen that when the target is symmetrically seen from the transmitter, the symmetry is also observed on the RCS variations around the orientation 0-degree.

Finally, in Fig. 10 we report the variation of the BRCS maxima as a function of the conducting strip width normalized to wavelength for different thicknesses in the case of horizontal incidence ($\phi_0 = \pi/2$).

5. CONCLUSION

In this paper, the synthesis procedure is computer simulated, and the corresponding data are presented. Using the surface impedance approach and the quasi-TEM approximations with a suite choice of basis and test functions, it is possible to calculate the surface current induced by the illuminating electromagnetic field. The scattered field is then calculated, and the problem of calculating the RCS is treated in detail. To illustrate the procedure, a lossy rectangular strip is considered for bistatic and monostatic RCS calculations. The numerical computation results are given for several cases and

compared with those obtained making use of a previous surface impedance version, HFSS and CST. The combination of the proposed method based on the surface impedance technique with the quasi-TEM analysis provides accurate results that agree very well with those provided by the more involved full-wave simulators in more practical situations.

REFERENCES

1. Balanis, C. A., *Antenna Theory: Analysis and Design*, John Wiley & Sons, 1997.
2. Eugene, F. K., *Radar Cross Section Measurements*, Spring US, 1993.
3. Shaeffer, J. F., M. T. Tuley, and E. F. Knot, *Radar Cross Section*, Artech House, 1985.
4. Skolnik, M. I., *Introduction to Radar Systems*, McGraw Hill, 1985.
5. Barton, D. K., *Modern Radar System Analysis*, Artech House, 1988.
6. Nathanson, F. E., *Radar Design Principles*, 2nd edition, McGraw Hill, 1991.
7. Meikle, H. D., *Modern Radar Systems*, Artech House, 2001.
8. Brookner, E., *Aspects of Modern Radar*, Artech House, 1998.
9. Kingsley, S. and S. Quegan, *Understanding Radar Systems*, McGraw Hill, 1992.
10. Skolnik, M., *Radar Handbook*, 2nd edition, McGraw-Hill, 1990.
11. Harrington, R. F., *Field Computation by Moment Methods*, IEEE Press, New York, 1993.
12. Bancroft, R., *Understanding Electromagnetic Scattering Using the Moment Method*, Artech House, London, 1996.
13. Hatamzadeh-Varmazyar, S., M. Naser-Moghadasi, and Z. Masouri, "A moment method simulation of electromagnetic scattering from conducting bodies," *Progress In Electromagnetics Research*, Vol. 81, 99–119, 2008.
14. Sevgi, L., *Electromagnetic Modeling and Simulation*, IEEE Press Wiley, 2014.
15. Hamham, E. M., F. Mesa, F. Medina, and M. Khalladi, "A surface-impedance Quasi-TEM approach for the efficient calculation of conductor losses in multilayer single and coupled microstrip lines," *IET, Microwaves, Antennas & Propagation*, Vol. 6, No. 5, 519–526, 2012.
16. Hamham, E. M., "Application of Quasi-TEM surface impedance approach to calculate inductance, resistance and conductor losses of multiconductor microstrip line system," *Progress In Electromagnetics Research M*, Vol. 50, 85–93, 2016.
17. Hatamzadeh-Varmazyar, S. and M. Naser-Moghadasi, "New numerical method for determining the scattered electromagnetic fields from thin wires," *Progress In Electromagnetics Research B*, Vol. 3, 207–218, 2008.
18. Danesfahani, R., S. Hatamzadeh-Varmazyar, E. Babolian, and Z. Masouri, "A scheme for RCS determination using wavelet basis," *Int. J. Electron. Commun.*, Vol. 64, 757–765, 2010.
19. Pozar, D. M., *Microwave Engineering*, John Wiley & Sons, 2005.
20. Marqués, R., J. Aguilera, F. Medina, and M. Horno, "On the use of the surface impedance approach in the quasi-TEM analysis of lossy and superconducting strip lines," *Mic. Opt. Tech. Lett.*, Vol. 6, No. 7, 391–394, 1993.
21. Aguilera, J., R. Marqués, and M. Horno, "Quasi-TEM surface impedance approaches for the analysis of MIC and MMIC transmission lines, including both conductor and substrate losses," *IEEE Trans. Microw. Theory Tech.*, Vol. 43, No. 7, 1553–1558, 1995.